VERTICAL PLANE HIGH RECEIVED POWER USING ENERGY SAVING CLUSTERING ALGORITHM IN RADIO COMMUNICATION IN URBAN STREETS

R.Ramya[1], A. Antoni Doss[2]

[1]PG Student, Department Of Computer Science and Engineering, Tagore Engineering College
[2]Assistant Professor, Department Of Computer Science and Engineering, Tagore Engineering College

Abstract−**This paper presents vertical plane models for the real-time prediction of the received power from waves propagating through urban street .Today there has been a large increase in the usage of devices emitting electromagnetic radiation. This influences almost every aspect of day-to-day living. Especially, public systems of mobile telephony became common-place communication technology around the world. Network simulation tools are frequently used to analyze performance of MANET protocols and applications. They commonly offer only simple radio propagation models that neglect obstacles of a propagation environment. This wireless technology relies upon an extensive network of fixed antennas or base stations, exchanging information by means of radio frequency (RF) signals. The line-of-sight (LOS) and non-line-of-sight (NLOS) models presented here are based on the two-ray model and are used to predict the small-area average received power (i.e., long-term/shadow fading and distance-dependence). Radio channels are much more complicated to analyze than wired channels. There are large differences between simple paths with line of sight (LOS) and those which have obstacles like buildings or elevations between the sender and the receiver (Non Line of Sight (NLOS)). To implement a channel model generally two cases are considered: large-scale and their characteristics may change rapidly and randomly. These models have two adjustable parameters that account for clutter such as road traffic and pedestrians and for scattering from objects and buildings at street intersections, respectively. Validation of these models is performed with mobile-to-mobile measurements in ns-2. This paper presented the vertical plane wave propagation through energy efficient clustering algorithm to save energy and the simulation are performed in ns-2.**

Index Terms--- Chanel model, diffraction, LOS, MANET, NLOS, path loss, scattering, urban propagation, VANET.

I. INTRODUCTION

This work presents computationally efficient vertical plane models of received power for peer-to-peer(mobile- to-mobile),backhaul and access radio links Urban street canyon radio propagation is a powerful electromagnetic modeling tool for predicting the effects of buildings and terrain on the propagation of electromagnetic waves It predicts how the locations of the transmitters and receivers within an urban area affect signal strength. Wireless in Site models the physical characteristics of the rough terrain and urban building features, performs the electromagnetic calculations and then evaluates the signal propagation characteristics. Wireless-defining tools or imported from an external data file. Separate calculations for portions of the overall area may be specified by defining study areas. The calculations are made by shooting rays from the transmitters, and propagating them through the defined environment. These rays interact with environmental features and make their way to receivers. Interactions include reflections from feature faces, diffractions around objects and transmissions through features. Wireless in Site uses advanced high-frequency electromagnetic methods to provide accurate results over a frequency range from approximately 50 MHz to 100 GHz. The effects of path to the receiver are ev electric field. At each receiver location, contributions from arriving ray paths are combined and evaluated to determine predicted quantities such as electric and magnetic field strength, received power, interference measures, path loss, delay spread, direction of arrival, impulse response, electric field vs. time, electric field vs. frequency and power delay profile.The fundamental components on which WLAN is composed of, are access points (AP) and the mobile clients (MC), typically a laptop or a PDA with a WLAN card. While for wired network communications, Ethernet cables are laid down all over the building and subsequently different buildings are linked to each other by using fibre optics. In Wireless LAN, in order to make a network infrastructure APs are positioned at different place all over a building and also if needed in outdoors as well. Then mobile clients communicate with each other by first communicating to the access points and then to the outer world. A major principle of WLAN communication is that, network data is transmitted as modulated electromagnetic waves using antenna. When radio waves transmit or travel from one device to another there are several issues one has to highlight. The radio

energy attenuates as it propagates and when it passes through obstacles like glass, wood, concrete and metal surfaces. The mechanisms that occur when radio waves propagate: NLOS, reflection, diffraction and scattering. Scattering occurs when RF can reflect over obstacles which has rough surfaces and after reflecting the signal is dispersed which results in fading of signal. Mostly wireless network equipment is subject to IEEE standardization. The IEEE standards for wireless LAN s in Site's powerful site describe the specifications for the physical layer and the Wireless LAN Medium Access Control (MAC) Layer. The standards describe these layers in detail in order to allow maker to use it as a directive for manufacturing wireless LAN card.

II. MODELS FOR LOS AND NLOS LINKS

For radios operating in an urban environment with a locally rectangular street grid, as in Fig. 1, there are three types of radio links in the HP. LOS links arise when the mobiles are on the same straight section of a street. NLOS links arise when the mobiles are located on two streets that intersect, or are parallel to each other. For mobiles on intersecting streets, the radio signal propagating in the HP can reach the receiver after turning one corner. We call this radio link a one- turn link. When the mobiles are on parallel streets, the radio signal propagating from one to the other must turn two corners. We call this type of link a two-turn link. Other paths in the HP connect the mobiles in these three cases but involve turning more corners. Since turning a corner involves substantial loss in amplitude [16], these other paths are neglected. For one -turn and two-turn links, the two-ray model used for LOS links is modified to account for diffraction and scattering by vertical structures, such as lampposts and building corners.

A. LOS Links

In [5] and [13], the distance dependence of the received power for LOS transmitter (TX) and receiver (RX) was found to follow the two -ray model. This model coherently adds the electric fields of the direct unobstructed ray and ground reflected ray. For isotropic, matched antennas, the received power $P_{2\text{R}}(R)$ in watts is given by [12]
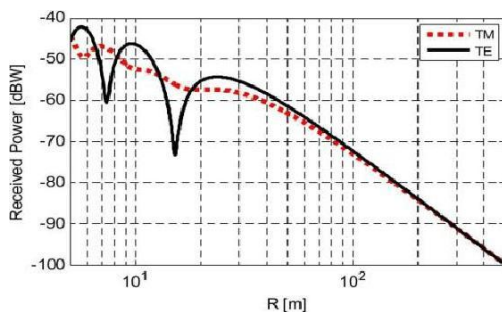
To account for the vehicular and pedestrian clutter, Oda and Tsunekawa [14], and Masui, *et al.* [15], [16] introduced an effective ground height h_G from which to measure the antenna height. They observed that the clutter on urban LOS links at midday caused the ground to appear to be between 1 m to 2 m higher than it was. They also observed that around midnight, when there was less traffic, the effective ground appeared to be only 0.5 m higher. The effective ground height serves as an adjustable parameter in our LOS and NLOS models and can be estimated from measurements or from results presented in [14]–[16].

$$P_{2\text{R}}(R) = P_{\text{TX}} \left(\frac{\lambda}{4\pi}\right)^2 \left| \frac{e^{-j2\pi\sqrt{R^2+(h_{\text{TX}}-h_{\text{RX}})^2}/\lambda}}{\sqrt{R^2 + (h_{\text{TX}} - h_{\text{RX}})^2}} + \Gamma(\theta)\frac{e^{-j2\pi\sqrt{R^2+(h_{\text{TX}}+h_{\text{RX}})^2}/\lambda}}{\sqrt{R^2 + (h_{\text{TX}} + h_{\text{RX}})^2}} \right|^2.$$

B. One-Turn NLOS Links

Radio signals can turn a corner from the street where the TX is located, to a cross street by means of reflection from building surfaces, and diffraction and/or scattering from building corners, lampposts, and other tall vertical structures in the street intersection. Reflection is important only near the intersection since reflected rays enter the side street at angles near normal to the buildings on the side street. Because of the near-normal incidence, reflected rays lose amplitude after a few reflections before traveling very far down the side street. In contrast, the diffracted and scattered rays experience significant loss from turning the corner but have a weak dependence on distance along the side street. This paper shows direct and ground-reflected rays diffracted at a vertical edge, such as the corner of a building. If the distance R_1+R_2 traveled by the rays along the ground from the TX antenna to RX antenna is large compared with the antenna heights h_{TX} and h_{RX}, then the diffraction loss at the corner will be nearly the same for both the direct and ground-reflected rays. Thus, for this pair of rays, diffraction will introduce an additional loss to the received power, such that,

$$P^{(1)} = P_{2\text{R}}(R_1 + R_2)\frac{|D|^2}{R_1 R_2}(R_1 + R_2).$$

Here, $P_{2\text{R}}(R_1+R_2)$ is the received power for distance R_1+R_2, and D is the diffraction coefficient of the edge. Note that when $R1$ and $R2$ are sufficiently large relative to the street widths, D can be approximated as a constant, because the diffraction angle approaches 90°.For a one-turn link in an urban environment, there are usually four corners at an intersection. In addition to corners, there may be tall vertical scatterers such as lampposts near the intersection.

Each scatterer will contribute two rays (direct and ground reflected) whose fields must be added coherently. The power from each ray pair is then expressed as in (2) with

$|D|^2$ replaced by a scattering coefficient.Ray pairs arriving from distinct directions produce a standing wave pattern whose small-area average power is the incoherent sum of the power carried by the individual ray pairs. Accordingly, for the average power of a one-turn link, the power Pi from the ray pair for the ith corner/scatterer is first found, and then summed incoherently over all i. Note that direct and ground-reflected rays of a pair are not separated because they arrive almost parallel from the same direction.Under the assumption that the TX and RX distances to and from the intersection are larger than the street width, the distance Rn from the TX antenna to the jth corner/scatterer can then be approximated as the distance Li from the TX antenna to the center of the intersection. Similarly, the distance R_{2i} from the ith corner/scatterer to the RX antenna can be approximated by the distance L_2 from the center of the intersection to the RX antenna. This assumption is equivalent to placing the vertical structures at the center of the intersection. Furthermore, instead of separately computing different diffraction and scattering coefficients for the individual corners and vertical scatterers, we employ a diffraction/scattering parameter S^2, which is the incoherent sum of the magnitude squared of the individual diffraction and scattering coefficients. The total average power P_{IT} can then be expressed as,

The parameter S is the second adjustable parameter in our models and is selected to describe the diffraction/scattering mechanisms at all intersections of a particular urban environment.

$$P_{1T} = \sum_i P_i^{(1)} \approx P_{2R}(L_1 + L_2) \frac{S^2}{L_1 L_2}(L_1 + L_2).$$

Fig. 3. Two-ray diffraction at a vertical edge.

C. Two-Turn NLOS Links

This model takes into consideration both direct and indirect paths between the transmitting and receiving node. This is an analytical model, which uses the following equation to calculate the approximately received power in watts.

$$P_r(d) = \frac{P_t G_t G_r h_t^2 h_r^2}{d^4 L} \quad \dots\dots 2.4$$

Where Pt is transmitted signal power, Gt and Gr are the transmitter and receiver antenna gains respectively, d is the distance between two communicating nodes, ht and hr are the transmitter and receiver antenna heights and L (L ≥ 1) is sources. For L=1, equation 2.4 can be expressed in dB as,

$$P_r dBm = P_t dBm + 10\log_{10}(G_t G_r) + 20\log_{10}(h_t h_r) - 40\log_{10}(d).$$

The two-ray model does not give good results for shorter distances due to oscillation caused by the constructive and destructive combination of the two rays. Free space path loss model based upon friis equation is a better choice for smaller distances ns-2 simulator uses a cross over distance d c when this model is used. If d ≤ d c , Friis equation and if d > dc, TRG model is used .At the cross over distance, both equations produce the same results, so dc can be calculated as

$$d_c = \frac{(4\pi h_t h_r)}{\lambda}.$$

Where λ is the wavelength (found reasonably accurate for predicting the large scale signal strength over distances of several kilometres for mobile radio systems that use tall towers (i.e. height which exceed 50 m), as well as for LoS microcell channels in urban environments.

ENERGY PREDICTION:

If effective communication over long distances were the only consideration, we might be concerned mainly with radiation of energy at the lowest possible angle above the horizon. However, being engaged in a residential avocation often imposes practical restrictions on our antenna projects. As an example, our 1.8 and 3.5-MHz bands are used primarily for short-distance communication because they serve that purpose with antennas that are not difficult or expensive to put up. Out to a few hundred miles, simple wire antennas for these bands do well, even though their radiation is mostly at high angles above the horizon. Vertical systems might be better for long-distance use, but they require extensive ground systems for good performance. Horizontal antennas that radiate well at low angles are most easily erected for 7 MHz and higher frequencies— horizontal wires and arrays are almost standard practice for work on 7 through 29.7 MHz. Vertical antennas are also used in this frequency range, such as a single omnidirectional antenna of multiband design. An antenna of this type may be a good solution to the space problem for a city dweller on a small lot, or even for the resident of an apartment building.In this project we are
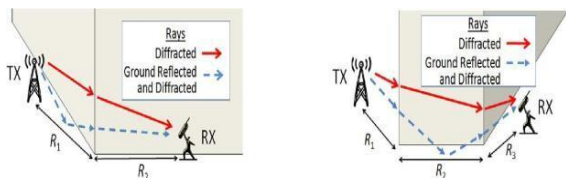
~

using perl scripting to identify the energy of the received signal strength to predictively manage the battery resource to the MANET An expression for the total small -area spatially averaged received power $P_{2\,\mathrm{All}}$ that considers all two-turn paths is where the superscript n denotes the nth two-turn path. From simulation results [26] not shown, only those two-turn paths whose L_2 segments lay inside or immediately outside the region between the TX and RX are important. Therefore, the summation in (6) can usually be truncated to include only a few two-turn paths.

III. MEASUREMENT OVERVIEW

Measurements were separately carried out in high-rise sec-tions of Denver [4] and New York [30] to simulate public- safety personnel walking through a high-rise urban environment while communicating with a mobile command center. As such, an operator carried single -frequency (continuous wave (CW)) transmitters (TXs) along the paths shown in Figs. 5 and 6, while receivers (RXs) at multiple locations recorded the received signal level.

A. Transmitter and Receiver Setup and Equipment

The transmitter part of the measurement system consisted of handheld CW TXs operating at $f =$ 430, 750, 905, 1834, 2400, and 4860MHz. The TXs had either linear dipole arrays or monopole antennas that radiated either 1-or 2-W nominal power P_{TX} . The P_{TX} and antenna gains G_{TX} for the different frequencies in each city are given in Table I. The TX antennas were always held at a height of $h_{\mathrm{TX}} \approx 1.5$ m and approximately 0.33 m away from the torso of the operator carrying them. The receiver part of the measurement system consisted of an antenna, spectrum analyzer, laptop, and controlling software. In Denver, the RX antennas were held by tripods $h_{\mathrm{RX}} = 2$ m high at four sites (RX1–RX4) denoted by the crosses in Fig. 5. For the New York City measurements, the RX antenna site is denoted by the cross

B. Description of TX Route and RX Locations

The measurement collections in Denver and New York City were performed during the daytime when there was significant vehicular traffic on the streets, as well as pedestrian traffic on the sidewalks. The TXs were carried on the sidewalks along the walking routes shown in Figs. 5 and 6. The RX antennas were positioned at four sites in Denver and one site in New York City. The numbering of the Denver RX sites used here differs from that used in [4]. The measurements reported in [4] also include an additional RX site and TX walking route located in a narrow pedestrian mall. Since the mall structure does not match that of a street, the measurements from those locations were not used in this study. The RX1 site was located on a sidewalk near a street intersection, while RX2 was located on a street 44 m from the center of the nearest street intersection. RX3 and RX4 were located in parking lots.

The blocks in the measurement areas had both rectangular and trapezoidal shapes so that the routes included corners that were not 90 ₒ , as seen for the corner near position 5 in Fig. 5and corners 3 and 4 in Fig. 6. Also, in Denver, the paths between some of the TX locations, and RX3 and RX4, which were in parking lots, turn corners of less than 90 ₒ . As will be shown in Section IV, our models provide good predictions even in the presence of such non ideal street configurations and corner angles.

C. Measurement Collection and Processing

The laptop and spectrum analyzer at the RX recorded a arrow frequency band (called the —capt around the nominal center frequency of the transmitted CW signal. The capture bandwidth was typically less than 20 kHz. The peak signal within the capture bandwidth was recorded as the measured CW signal power P_{RX}. As with similar urban RF propagation measurements, instrument measurement un-certainty is expected to be negligible relative to the RF channel variability [31]. The time resolution of the received signals was determined by the sampling rate of the complete measurement process. Sampling rates in Denver were 1 sample/s for all frequencies. Sampling rates in New York 3.3 and 5 samples/s for 905 and 1834 MHz, respectively. Accounting for a 1-m/s walking speed, the spatial separation of our Denver measurements was approximately 1 m. In New York, it was 0.3 and 0.2 m for 905 and 1834 MHz, respectively

IV. COMPARISON WITH DENVER MEASUREMENTS

In this section, the effective ground height h_G and diffraction/scattering parameter S are estimated from the isotopic loss-less measurements recorded at RX1 in Denver. To validate the received power models presented in Section II, predictions are computed from the models using the estimated h_G and S, and then compared with measurements recorded at RX2, RX3, and RX4.

A. Extracting the Effective Ground Height h_G

To extract h_G from the measurements, a 0-dB mean-error constraint was applied to LOS predictions from (1) for measurements recorded at RX1 when the TX antenna was within 60 m of RX1. Here, error is defined as the measured received power in decibel watts minus the predicted received power in decibel watts. Considering measurements at all frequencies listed in Table I, h_G was found to be 1.2 m, which is consistent with the findings in [14]–[16]. The value $h_G = 1.2$ m was used in the 750-MHz LOS predictions, plotted as the black solid curves in well, even

outside of our fitting range, that is, for distances greater than 60 m from the RX antenna. The mean LOS prediction error is 1.1 dB, and the standard deviation of the prediction error is 4.3 dB.

B.Extracting the Diffraction/Scattering Parameters

To extract a value of S for each frequency listed in Table I, a 0-dB mean- error constraint was again applied when comparing predictions computed with the one-turn model of (3) to the NLOS Denver measurements recorded at location RX1 in Fig. 5. Note that all NLOS measurements recorded at RX1 are one- turn, as seen in Fig. 5. The values found for S are [4.1, 2.9, 7.1, 6.4, 4.4, 2.8] at $f =$ 430, 750, 905, 1834, 2400, and 4860 MHz, respectively. As an example, the predictions from the one-turn model of (3) are plotted as the black dashed line in Fig. 7 using the zero-mean S for $f =$ 750 MHz. The mean deviation of the measurements from the model is 0 dB with 5.2-dB standard deviation.

C. Link Classification

In order to generate predictions for the various TX and RX antenna locations, the radio links must be classified as either LOS, one-turn or two-turn. This classification was performed visually for all TX antenna locations on the route shown in Fig. 5 and all RX antenna sites. For NLOS links to RX2, the turn locations were taken as the centers of the street intersections. To deter-mine the turn locations for NLOS links to RX3 and RX4, sections of the parking lots were treated as streets. As an example, the turn locations for RX3 are shown in Fig. 8. Four TX antenna locations are also shown in this figure. Each TX has a one-turn radio link with RX3. In the case of TX3 and TX4, the turn location is at the center of a street intersection, as denoted by the red dot. The distances L_1 and L_2 were measured from this point. For TX1 and TX2, sections of the propagation paths were taken along the inner boundaries of the parking lot, as shown in Fig. 8,

D. Comparison of Model Predictions to RX2, RX3, RX4 Measurements

To show that only a limited number of measurements are needed for accurate characterization of LOS and NLOS propagation in urban street canyons, the values of h_G and S extracted from the RX1 measurements were used to predict the received power recorded at RX2, RX3. Predictions for LOS links are shown as thick solid black curves, while those for one-turn links and two-turn links are shown as dashed and dotted black colored curves, respectively. The predictions and measurements generally compare well in the prediction of the distance dependence, even near to the intersections. In addition, predictions using the value of h_G and S extracted from one-turn measurements recorded at RX1,To quantitatively characterize the accuracy of our models, prediction error

statistics are computed. A focus is placed on the NLOS model results. The LOS model accuracy has been well characterized in [5], [13]–[16] and is seen to compare well with our 750-MHz measurements in Figs. 7 and 9(a)–(c) with 1.9 -dB mean error and 4-dB standard deviation of error calculated over all RX sites.

V. CHARACTERIZING THE DIFFRACTION/SCATTERING PARAMETER

In the previous section, measurements record at RX2, RX3, and RX4 were compared with predictions made using the values of h_G and S extracted from measurements at RX1. In this section, measurements recorded at RX2, RX3, and RX4 were re-processed to extract values of using the 0-dB mean-error criterion and $h_G =$ 1.2 m, as in Section IV.MHz and 1834 MHz were similarly processed to obtain values of S using $h_G =$ 1.33 m. The resulting values of S are also listed in Table III. An example of the New York measurements and predictions for the $f =$ 1834 MHz are given in Fig. 11. Again, the LOS and NLOS models are seen to com-pare well with the small-area-averaged measurements. This further supports our approach in which a single value for S is used for the NLOS power predictions in a city. On the other hand, for different cities, the S values at a specific frequency may vary. This may be due to the street furniture [24], [25], building architecture [32], and/or block layout unique to each environment.

To develop a model for S, the values in were scatter-plotted in decibels versus $\log(f)$. A least-squares error fi t to the scatter plot was then computed to obtain the power law dependence on f in hertz. The resulting dependence in linear terms is Note that if diffraction at building corners is the only propagation mechanism by which a signal turns a corner, then the theory of diffraction by a wedge suggests that the frequency dependence should be f_{-05}, rather than the weak dependence in (8). However, as discussed previously, the signal may also turn the corner as a result of

scattering at lampposts and other vertical objects [24], [25]. In [24], results show that the contribution of scattering from a single lamppost can be equal to that due to diffraction from four corners. For UHF frequencies, the scattering cross section of a cylindrical metal lamppost is approximately frequency independent [29], which may explain the weak frequency dependence in (8).

VI. CONCLUSION

In this paper, we presented computationally efficient urban propagation models to compute the horizontal-plane contribu-tion to the total power for LOS and NLOS radio links in urban environments. Because the horizontal-plane contribution is dominant in high-rise urban environments, we have validated these models against measurements conducted in the high-rise portions of Denver and New

York City over a wide range of frequencies.The LOS and NLOS models presented here require minimal information about the environment: 1) link classification and 2) pertinent distances for the models, i.e., R, L_1, L_2, and L_3. Our models use two site- specific empirical parameters to account for the clutter in the streets such as pedestrians and vehicles,and diffraction and scattering near street intersections, respec-tively. The effective ground height h_G accounts for the clutter and is frequency independent, with values of 1.2 m in Denver and 1.33 m in New York City. The diffraction/scattering param-eter S accounts for the site-specific vertical features in and near the street intersections, such as corner composition, lampposts, and acute corner angles, and has values ranging from 1.7 to 7.1. Comparisons show that at the same frequency and city, values of S are fairly consistent.For cases in which NLOS measurements are not readily avail-able, we have developed a simple frequency dependent model for S. It remains to develop a more complete model of S that accounts for other site-specific features, such as street width and corner construction. As discussed, the models presented here only consider waves propagating in the horizontal plane. These models have been shown to be sufficient for power prediction in high-rise urban environments.

REFERENCES

[1] I. K. Eltahir, "The impact of different radio propagation models for mo-bile ad hoc networks (MANET) in urban area environment," presented at the Wireless Broadband and UWM Comm. Conf., Sydney, Australia, Sep. 2007.

[2] ECC, "Technical and operational requirements for the possible oper-ation of cognitive radio systems in the white spaces of the frequency band 470–790 MHz," ECC meeting, Cardiff, Wales, 2011, ECO WG SE43, ECC Rep. 159.

[3] J. Punnoose, P. V. Nikitin, J. Broch, and D. D. Stancil, "Optimizing wireless network protocols using real-time predictive propagation modeling," in *Proc. Radio Wireless Conf. (RAWCON)*, Aug. 1999, pp. 39–44.

[4] D. W. Matolak, Q. Zhang, and Q. Wu, "Path loss in an urban peer-to-peer channel for six public-safety frequency bands," *IEEE Wireless Commun. Lett.*, vol. 2, no. 3, pp. 263–266, 2013.

[5] J. R. Hampton, N. M. Merheb, W. L. Lain, D. E. Paunil, R. M. Shu-ford, and W. T. Kasch, "Urban propagation measurements for ground based communication in the military UHF band," *IEEE Trans. An-tennas Propag.*, vol. 54, no. 2, pp. 644–654, Feb. 2006.

[6] C. Phillips, D. Sicker, and D. Grunwald, "Bounding the error of path loss models," in *Proc. IEEE Symp. New Frontiers Dynam. Spectrum Access Netw. (DySPAN)*, May 2011, pp. 71–82.

[7] G. E. Athanasiadou, A. R. Nix, and J. P. McGeehan, "A microcellular ray-tracing propagation model and evaluation of its narrow-band and wide-band predictions," *IEEE J. Sel. Areas Commun.*, vol. 18, no. 3, pp. 322–335, Mar. 2000.

[8] K. Rizk, J. F. Wagen, and F. Gardiol, "Two-dimensional ray-tracing modeling for propagation prediction in microcellular environments," *IEEE Trans. Veh. Technol.*, vol. 46, no. 2, pp. 508–518, May 1997.

[9] T. Kürner, D. J. Cichon, and W. Wiesbeck, "Concepts and results for 3D digital terrain-based wave propagation models: An overview," *IEEE J. Sel. Areas Commun.*, vol. 11, no. 7, pp. 1002–1012, Sep. 1993.

[10] K. Rizk, R. Valenzuela, S. Fortune, D. Chizhik, and F. Gardiol, "Lat-eral, full-3D and vertical plane propagation in microcells and small cells," in *Proc. IEEE Veh. Technol. Conf.*, 1998, pp. 998–1003.

[11] H. L. Bertoni, *Radio Propagation for Modern Wireless Applications*. Upper Saddle River, NJ, USA: Prentice-Hall, PTR, 2000.

[12] H. H. Xia, H. L. Bertoni, L. R. Maciel, A. Lindsy-Stewart, and R. Rowe, "Radio propagation characteristics for line-of-sight microcel-lular and personal communications," *IEEE Trans. Antennas Propag.*, vol. 41, no. 10, pp. 1439–1447, 1994.

[13] Oda and K. Tsunekawa, "Advanced LOS path loss model in mi-crowave mobile communications," in *Proc. IEEE Ant. Propag. Conf.*, Apr. 1997, vol. 2, pp. 170–173.

[14] H. Masui, M. Ishii, K. Sakawa, H. Shimizu, T. Kobayashi, and M. Akaike, "Microwave propagation characteristics in an urban LOS environment in different traffic conditions," in *Proc. IEEE Antennas Propag. Symp.*, 2000, pp. 1150–1153.

[15] H. Masui, M. Ishii, K. Sakawa, H. Shimizu, T. Kobayashi, and M. Akaike, "Microwave path-loss characteristics in urban LOS and NLOS," in *Proc. IEEE Veh. Technol. Conf.*, 2001, pp. 395–398.

[16] J. H. Tarng and K. M. Ju, "A novel 3-D scattering model of 1.8-GHz radio propagation in microcellular urban environment," *IEEE Trans. Electromagn. Compat.*, vol. 41, no. 2, pp. 100–106, 1999.

[17] M. R. J. A. E. Kwakkernaat and M. H. A. J. Herven, "Analysis of scattering in mobile radio channels based on clustered multipath es-timates," *Int. J. Wireless Inf. Netw.*, Mar. 24, 2009, 10,1007/s10776-009-0096-y.

[18] V. Erceg, S. Ghassemzadeh, M. Taylor, D. Li, and D. L. Schilling, "Urban, suburban out-of-sight propagation modeling," *IEEE Commun. Mag.*, vol. 30, no. 6, pp. 56–61, Jun. 1992.

[19] H. M. El-Sallabi, "Fast path loss prediction by using virtual source technique for urban microcells," in *Proc. IEEE Veh. Technol. Conf.*, 2000, vol. 3, pp. 2183–2187.

[20] S. Y. Tan and H. S. Tan, "Propagation model in an urban street scene for microcellular communications," *IEEE Trans. Electromagn. Compat.*, vol. 35, no. 4, pp. 423–428, Nov. 1993.

[21] V. Erceg, A. J. Rustako, and R. S. Roman, "Diffraction around corners and its effects on the microcell coverage area in urban and suburban en-vironments at 900 MHz, 2 GHz and 6 GHz," *IEEE Trans. Veh. Technol.*, vol. 43, no. 3, pp. 762–766, Aug. 1994.

[22] J. Lee and H. L. Bertoni, "Coupling at cross, T and L junctions in tun-nels," *IEEE Trans. Antennas Propag.*, vol. 51, no. 5, pp. 926–935, May 2003.

[23] K. Rizk, J. F. Wagen, J. Li, and F. Gardiol, "Lamppost and panel scat-tering compared to building reflection and diffraction," in *Proc. COST 259*, May 1996.

[24] M. Ghoraishi, J. Takada, and T. Imai, "Identification of scattering ob-jects in microcell urban mobile propagation channel," *IEEE Trans. An-tennas Propag.*, vol. 54, no. 11, pp. 3473–3480, Nov. 2006.

[25] J. S. Lu, "Simplified urban propagation models for rapid computation of site-specific path gain," Master's thesis, Polytechnic Institute, New York Univ., New York, NY, USA, May 2010, partial

fulfillment of MS/EE.

[26] F. Niu and H. L. Bertoni, "Path loss and cell coverage of urban mi-crocells in high-rise building environments," in *Proc. IEEE Global Telecommun. Conf. (GLOBECOM)*, Nov. 1993, vol. 1, pp. 266–270.

[27] D. A. McNamara, C. W. I. Pistorius, and J. A. G. Malherbe, *Introduc-tion to the Uniform Geometrical Theory of Diffraction*. Boston, MA,
USA: Artech House, 1990.

[29] C. A. Balanis, *Advanced Engineering Electromagnetics*, 2nd ed. Hoboken, NJ, USA: Wiley, 2012.

[30] W. F. Young, K. A. Remley, C. Koepke, D. Cameil, and J. Healy, "Performance analysis of RF-Based electronic safety equipment on a subway station and the Empire State Building," NIST, Boulder, CO, USA, NIST Tech. Note 1792, Mar. 2013.

[31] W. F. Young, K. A. Remley, D. W. Matolak, Q. Zhang, C. L. Holloway,

C. Grosvenor, C. Gentile, G. Koepke, and Q. Wu, "Measurements and models for the wireless channel in a ground-based urban setting in two public safety frequency bands," NIST, Boulder, CO, USA, NIST Tech. Note 1557, Jan. 2011.

[32] H. M. El-Sallabi, G. Liang, H. L. Bertoni, I. T. Rekanos, and P. Vainikainen, "Influence of diffraction coefficient and corner shape on ray prediction of power and delay spread in urban microcells," *IEEE Trans. Antennas Propag.*, vol. 50, no. 5, pp. 703–712, May 2002.

[33] C. Chrysanthou, J. K. Breakall, K. L. Labowshki, S. G. Bilen, and W.
Glessner, "A simplified analytical Urban Propagation Model (UPM) for use in CJSMPT," in *Proc. IEEE Military Commun. Conf.*, Oct. 2007